

Assessing the causal effects of a stochastic intervention in time series data: Are heat alerts effective in preventing deaths and hospitalizations?

XIAO WU^{1,4,*}, KATE R. WEINBERGER², GREGORY A. WELLENIUS³, FRANCESCA DOMINICI⁴,

DANIELLE BRAUN⁴

¹Stanford Data Science and Department of Statistics, Stanford University, Stanford, CA 94305, USA

²School of Population and Public Health, University of British Columbia, Vancouver, BC V6T 1Z3, Canada

³Department of Environmental Health, Boston University School of Public Health, Boston, MA 02118, USA

⁴Department of Biostatistics, Harvard T.H. Chan School of Public Health, Boston, MA 02115, USA

*wuxiao@stanford.edu

SUMMARY

The methodological development of this paper is motivated by the need to address the following scientific question: does the issuance of heat alerts prevent adverse health effects? Our goal is to address this question within a causal inference framework in the context of time series data. A key challenge is that causal inference methods require the overlap assumption to hold: each unit (i.e., a day) must have a positive probability of receiving the treatment (i.e., issuing a heat alert on that day). In our motivating example, the overlap assumption is often violated: the probability of issuing a heat alert on a cool day is zero. To overcome this challenge, we propose a *stochastic intervention* for time series data which is implemented via an incremental time-varying propensity score (ItvPS). The ItvPS intervention is executed by multiplying the probability of issuing a heat alert on day t – conditional on past information up to day t – by an odds ratio δ_t . First, we introduce a new class of causal estimands that relies on the ItvPS intervention. We provide theoretical results to show that these causal estimands can be identified and estimated under a weaker version of the overlap assumption. Second, we propose nonparametric estimators based on the ItvPS and derive an upper bound for the variances of these estimators. Third, we extend this framework to multi-site time series using a meta-analysis approach. Fourth, we show that the proposed estimators perform well in terms of bias and root mean squared error via simulations. Finally, we apply our proposed approach to estimate the causal

effects of increasing the probability of issuing heat alerts on each warm-season day in reducing deaths and hospitalizations among Medicare enrollees in 2,837 U.S. counties.

Key words: Incremental propensity score; Meta-analysis; Multi-site time series; Time-varying confounding

1. INTRODUCTION

Extreme heat events are a significant threat to public health (US EPA, 2006). In the U.S., heat waves have been associated with increased morbidity and mortality (Bobb *and others*, 2014; Weinberger *and others*, 2020). To reduce heat-related adverse health outcomes, the U.S. National Weather Service (NWS) issues excessive heat warnings (to indicate more severe heat events) and heat advisories (to indicate less severe heat events) in advance of forecasted heat events to communicate these risks to the public and local government officials (Hawkins *and others*, 2017). However, how effective these excessive heat warnings and advisories (collectively, “heat alerts”) are in reducing adverse health outcomes such as deaths and hospitalizations is largely unknown (Weinberger *and others*, 2021). To fill these knowledge gaps, we acquired daily time series data during the warm months (April-October) of 2006-2016 for $N = 2,837$ U.S. counties. For each county, we obtained 1) daily maximum heat index (an index that combines air temperature and relative humidity to posit a human-perceived equivalent temperature); 2) daily issuance of heat alerts (binary); and 3) daily number of deaths and hospitalizations among Medicare enrollees. We define the unit of analysis as *the day* to align with the time series literature in environmental epidemiology (Bhaskaran *and others*, 2013).

To analyze this data set within a causal inference framework, we need to overcome the following methodological challenges. First, the overlap assumption (Rosenbaum and Rubin, 1983), i.e., any day must have a positive probability of being treated (e.g., receiving a heat alert) or untreated (e.g., not receiving a heat alert), is often violated in time series data. This is because during the study period heat alerts were only issued on 2.52% of the warm-season days across U.S. counties. Moreover, a heat alert is highly unlikely on a cool day, and more likely on a very hot day. Even if the overlap assumption did hold, unrealistically large sample sizes would be needed to avoid point estimates of the causal effects with very large estimated variances (Kang *and others*, 2007). Second, time series observational studies are prone to time-varying confounding. To adjust for confounding bias, we must control for time-varying covariates (e.g., daily maximum heat index) associated with both the treatment (e.g., daily issuance of heat alerts) and outcomes of interest (e.g., daily

deaths or hospitalizations). Third, we are dealing with multi-site time series data where it is plausible that the true causal effects of interest (e.g., whether heat alerts prevent deaths and hospitalizations in a given county) might be highly heterogeneous across counties.

Previous literature has focused on some aspects of the methodology gaps identified above. First, while the causal inference literature on time series studies is sparse, there are a few exceptions (Bojinov and Shephard, 2019; Papadogeorgou *and others*, 2020). Bojinov and Shephard (2019) introduced an extended potential outcome framework for randomized experiments on time series data assuming the overlap assumption always holds. They focused on the setting where the treatment at each time can be randomly assigned based on positive probabilities, and therefore their work does not directly apply to time series observational studies with overlap violations. Second, stochastic interventions (e.g., increasing or decreasing the probability of issuing heat alerts on each day), have been proposed to overcome violations of the overlap assumption in observational studies (Haneuse and Rotnitzky, 2013; Kennedy, 2019; Imai and Jiang, 2019; Naimi *and others*, 2021). Most recently, Kim *and others* (2019) proposed a causal inference framework based on stochastic interventions accounting for time-varying confounding in longitudinal studies. However, there are important distinctions between longitudinal studies and multi-site time series studies. More specifically, in longitudinal studies, the number of study units, which are often defined by individual patients or sites (N), is much larger than the number of repeated observations (T) for each study unit ($T \ll N$). Whereas, in multi-site time series studies, the number of study units, which are instead defined by time points (e.g., days T), can be larger than the number of sites (e.g., counties N). Such distinctions in data structure lead to different considerations in defining causal estimands and developing statistical methods. Papadogeorgou *and others* (2020) are the first to bridge a stochastic intervention with time series observational data, but they focused on treatments that can be modeled by a spatio-temporal point process. In this context, they analyzed a single time series that contains information on the geographic coordinates of treatments (e.g., airstrikes). In the presence of heterogeneity of the true causal effects across counties, as is the case in our motivating example, the causal estimands defined on a homogeneous super-population – as is done in the context of longitudinal studies or for a spatio-temporal point process – might not capture the heterogeneous nature of the study population.

To the best of our knowledge, a causal inference approach in the context of a stochastic intervention for

multi-site time series is lacking. Accordingly, in this paper, we introduce a stochastic intervention defined by the incremental time-varying propensity score (ItvPS) for time series data (i.e., the ItvPS intervention). The ItvPS intervention is executed by multiplying the probability of receiving the treatment at time t conditional on past information up to time t by an odds ratio δ_t (e.g., increase the probability of issuing heat alerts on day t). This novel framework allows us to define a broad class of stochastic causal estimands on time series data and ease the identification and estimation due to the violation of overlap assumption.

In Section 2, we discuss the motivating example which includes national data on heat alerts, heat index, and Medicare death and hospitalization records. In Section 3, starting in the context of a single time series, we define the stochastic causal estimands based on ItvPS intervention and their corresponding assumptions of identifiability. Next, in Section 4, we propose nonparametric estimators based on ItvPS, derive an upper bound for the variances of these estimators, and construct the corresponding asymptotic confidence intervals (CIs). In Section 5, we extend our approach into the context of multi-site time series, introduce additional assumptions of identifiability for multi-site time series, and propose a random-effects meta-analysis to pool causal estimands across time series from multiple sites. In Section 6, we illustrate the finite-sample performance of the proposed estimators via simulation studies. In Section 7, we apply our method to the national heat alert data set to estimate the effectiveness of heat alerts in reducing morbidity and mortality among Medicare beneficiaries. In Section 8, we conclude with a summary and discussion.

2. SET UP

2.1 *Mathematical Notations*

We introduce the following notation in the context of time series data. Let $Y_{i,t}, W_{i,t}, \mathbf{C}_{i,t}$ be the outcome, treatment and pre-treatment covariates at time t , respectively, for $t \in \{1, 2, \dots, T\}$ in site i , for $i \in \{1, 2, \dots, N\}$. First, we introduce the causal estimands in the context of a single time series, and omit the index i for conciseness. Later, in Section 5, we reintroduce the index i to indicate multiple time series across multiple sites.

For a single time series, each time t can be assigned to the treatment $W_t = 1$ or $W_t = 0$, and then the outcome Y_t is observed. We assume that W_t is binary; Y_t and \mathbf{C}_t can be binary, categorical or continuous. We define $\{\mathbf{C}_{1:T} = (\mathbf{C}_1, \dots, \mathbf{C}_T), W_{1:T} = (W_1, \dots, W_T), Y_{1:T} = (Y_1, \dots, Y_T)\}$. We denote by \mathcal{F}_t the

filtration which is used to capture past information prior to the treatment assignment at time t , that is $\mathcal{F}_t = \{\mathbf{C}_{1:t}, W_{1:(t-1)}, Y_{1:(t-1)}\}$ (note, \mathbf{C}_t is defined as pre-treatment covariates at time t and therefore $\mathbf{C}_{1:t}$ is included in the filtration \mathcal{F}_t and not $\mathbf{C}_{1:(t-1)}$). Following the potential outcome framework for time series data (Bojinov and Shephard, 2019), we denote $Y_t(w_{1:t})$ the potential outcome at time t that would have been observed under the treatment path $w_{1:t} = (w_1, \dots, w_t)$, and we introduce the potential outcome path $Y_{1:t}(w_{1:t}) = \{Y_1(w_{1:1}), Y_2(w_{1:2}), \dots, Y_t(w_{1:t})\}$.

We define the time-varying propensity score at time t as

$$p_t(w_t, \mathcal{F}_t) = Pr(W_t = w_t | \mathcal{F}_t), \text{ for } w_t = \{0, 1\}.$$

In our motivating example, the time-varying propensity score for treatment $W_t = 1$ denotes the probability of issuing a heat alert on day t conditional on past information up to day t prior to the heat alert issuance.

We extend the incremental propensity score intervention proposed by Kennedy (2019) to the time series studies. First, we introduce the notation of the ItvPS as:

$$p_t^{\text{ItvPS}}(w_t, \mathcal{F}_t) := \frac{w_t \delta_t p_t(1, \mathcal{F}_t) + (1 - w_t) \{1 - p_t(1, \mathcal{F}_t)\}}{\delta_t p_t(1, \mathcal{F}_t) + 1 - p_t(1, \mathcal{F}_t)}, \text{ for } w_t = \{0, 1\}. \quad (2.1)$$

where δ_t is, by definition, an odds ratio:

$$\delta_t = \frac{p_t^{\text{ItvPS}}(1, \mathcal{F}_t) / \{1 - p_t^{\text{ItvPS}}(1, \mathcal{F}_t)\}}{p_t(1, \mathcal{F}_t) / \{1 - p_t(1, \mathcal{F}_t)\}}. \quad (2.2)$$

Next, we define a stochastic intervention by the notation of ItvPS, and call it an ItvPS intervention. By executing an ItvPS intervention, we replace the probability of receiving the treatment $p_t(1, \mathcal{F}_t)$ at time t by $p_t^{\text{ItvPS}}(1, \mathcal{F}_t)$. Such a stochastic intervention reflects an odds ratio change of δ_t in the time-varying propensity scores. In the policy-relevant question, this can be explained as multiplying the probability of receiving the treatment on day t – conditional on past information up to day t (i.e., \mathcal{F}_t) – by an odds ratio δ_t (see Equation 2.2).

In the context of a time series with length T , we denote $\delta_{1:T} = \{\delta_1, \delta_2, \dots, \delta_T\}$ as the whole intervention path and $w_{1:T}^{\text{ItvPS}}(\delta_{1:T})$ as the post-intervened treatment path under the intervention path $\delta_{1:T}$.

2.2 Motivating Example

It is helpful to illustrate these mathematical notations in our motivating example. The binary treatment W_t indicates the issuance of a heat alert on day t in a given county. The covariates \mathbf{C}_t include (forecasted)

population-weighted daily maximum heat index that occurred just prior to treatment on day t , day of the week, and federal holidays which may be related to both heat alert issuance and adverse health outcomes (Weinberger *and others*, 2021). The outcome Y_t denotes the daily number of all-cause deaths or the daily number of cause-specific hospitalizations for each of five disease causes that were found to be associated with extreme heat in the Medicare population (heat stroke, urinary tract infections, septicemia, renal failure, fluid and electrolyte disorders; Bobb *and others* (2014)). Note, we do not have information on cause-specific deaths, therefore we focus on all-cause deaths. The filtration \mathcal{F}_t represents the past information prior to the treatment assignment on day t . The inclusion of past treatments $W_{1:t-1}$ and/or outcomes $Y_{1:t-1}$ is also allowed through the filtration, aligning with other literature (Bojinov and Shephard, 2019; Kennedy, 2019).

While the exact criteria used to issue heat alerts varies across the jurisdictions of local NWS offices, a key commonality across jurisdictions is that the issuance of heat alerts is based on forecasts of future weather conditions based on past information. Therefore, the probability of issuing a heat alert on day t , $p_t(w_t, \mathcal{F}_t)$ is modeled based on the past information \mathcal{F}_t as discussed in the previous paragraph.

If we consider a hypothetical ItvPS intervention in Los Angeles County, where one could increase the probability of issuing heat alerts by an odds ratio $\delta_t = 10$ for every day t during the warm months (April-October) of 2006-2016. Figure 1 illustrates the comparison between the heat alerts that have been issued and the heat alerts that could have been issued under this ItvPS intervention. For example, if the probability of issuing a heat alert on day t is 90%, under the stochastic intervention with $(\delta_t = 10)$, the counterfactual probability of issuing a heat alert would increase to $\frac{10 \times 90\%}{10 \times 90\% + 1 - 90\%} \approx 98.9\%$. It is worth clarifying that increasing the probability of issuing a heat alert by an odds ratio of 10 for each day is not equivalent to increasing the total number of heat alerts by 10 times. We find that if we hypothetically increase the probability of issuing a heat alert by an odds ratio 10 on each warm-season days, the NWS office would have issued 128 heat alerts (an average of approximately 12 alerts per year) in the warm months of 2006-2016, compared to the total of 56 heat alerts (an average of approximately 5 alerts per year) actually issued.

3. CAUSAL ESTIMAND AND IDENTIFICATION

3.1 General Estimand

We focus on the following scientific question “If we had changed the probability of issuing heat alerts by some pre-specified amount on each day in the study period, how many total deaths would have been

averted and how many cause-specific hospitalizations for heat-related diseases could have been avoided?” This question can be answered by quantifying the causal effect of an ItvPS intervention. We first define the general causal estimand of an ItvPS intervention in the context of time series data. The parameter $\tau_t(\delta_{1:t}) := E[Y_t\{w_{1:t}^{\text{ItvPS}}(\delta_{1:t})\}]$ denotes the mean potential outcome at time t with respect to the post-intervened treatment path $w_{1:t}^{\text{ItvPS}}(\delta_{1:t})$. In econometrics, this parameter belongs to the class of dynamic causal effects since the parameter changes over time (Rambachan and Shephard, 2021). In our motivating example, this would be the counterfactual daily deaths or hospitalizations on day t given the ItvPS intervention.

In cross-sectional or longitudinal studies, causal estimands are generally defined as the average of potential outcomes across N patients or location sites. In the context of a single time series, we define the causal estimand as the temporal average of the potential outcomes up to time T . Under the post-intervened treatment path $w_{1:t}^{\text{ItvPS}}(\delta_{1:t})$ where the probability of receiving the treatment on day t has been multiplied by an odds ratio δ_t for $t = 1, \dots, T$, we define following temporal-average causal estimand

$$\bar{\tau}(\delta_{1:t,T}) = \frac{1}{T} \sum_{t=1}^T \tau_t(\delta_{1:t}).$$

In our motivating example, for Los Angeles County (see Figure 1), the parameter $\bar{\tau}(\delta_{1:t,T})$ denotes the average number of deaths or cause-specific hospitalizations per day under the hypothetical scenario where the probability of issuing a heat alert is multiplied by an odds ratio $\delta_t = 10$ for each day $t = 1, \dots, T$ during the warm season.

3.2 Causal Estimand on Observed Treatment Path

Without further modeling assumptions, estimating the causal estimand $\bar{\tau}(\delta_{1:t,T})$ defined in Section 3.1 might be challenging for large T because this parameter depends on a treatment path with length T . Building upon Bojinov and Shephard (2019), we define a duration- t_0 causal estimand conditional on the observed treatment path $w_{1:(t-t_0-1)}^{\text{obs}}$ denoted as $\tau_t(\delta_{(t-t_0):t})$ (i.e., the duration of interventions is up to t_0 days), and its temporal average $\bar{\tau}(\delta_{(t-t_0):t,T})$, as follows

$$\begin{aligned} \tau_t(\delta_{(t-t_0):t}) &= E[Y_t\{w_{1:(t-t_0-1)}^{\text{obs}}, w_{(t-t_0):t}^{\text{ItvPS}}(\delta_{(t-t_0):t})\}], \quad t_0 = 0, \dots, t-1; \\ \bar{\tau}(\delta_{(t-t_0):t,T}) &= \frac{1}{T-t_0} \sum_{t=t_0+1}^T \{\tau_t(\delta_{(t-t_0):t})\}. \end{aligned}$$

By making the estimands dependent on the observed treatment path $w_{1:(t-t_0-1)}^{obs}$, we define causal estimands that can be estimated nonparametrically (see Section 4). The use of duration- t_0 causal estimands are consistent with time series models with pre-specified fixed memory (e.g., autoregressive integrated moving average (ARIMA) model). They are also compatible with the causal inference literature since they can be treated as conditional causal estimands conditioning on partial historical information $\{W_{1:(t-t_0-1)} = w_{1:(t-t_0-1)}^{obs}\}$ (Imbens and Rubin, 2015).

3.3 Assumptions and Identification

Following the potential outcomes framework for time series data (Bojinov and Shephard, 2019), we introduce the following assumptions of identifiability:

Assumption 1 (SUTVA) The outcome path satisfies non-anticipating and consistency assumptions, that is,

$$Y_t^{obs} = Y_t(w_{1:T}^{obs}) = Y_t(w_{1:t}^{obs}) \quad \forall t = 1, \dots, T.$$

Assumption 1 generalizes the Stable Unit Treatment Value (SUTVA) assumption (Imbens and Rubin, 2015) to allow for the potential outcomes at time t to depend on the treatment path up to time t , but the potential outcomes are not allowed to depend on future treatments (non-anticipating). We also assume that there is only one version of the treatment for each time t , and each treatment path up to time t realizes a unique observed outcome at time t (consistency).

Assumption 2 (Unconfoundedness) The assignment mechanism is unconfounded if for all $W_{1:T} \in \mathcal{W} = \{0, 1\}^T$,

$$W_t \perp Y_s(w_{1:s}) \mid \mathcal{F}_t \quad \forall t = 1, \dots, T \text{ and } t \leq s \leq T.$$

Assumption 2 aligns with the “sequential randomization” assumption introduced in longitudinal studies by Robins *and others* (1994), which states that the treatment assignment only depends on the past information and thus is conditionally independent of future potential outcomes. This assumption also excludes the possibility that future potential outcomes could impact the current treatment assignment retrospectively (a phenomenon that has been discussed in Granger (1980)).

Assumption 3 (Weak overlap) The assignment mechanism weakly overlaps if for all $t \in \{1, 2, \dots, T\}$, there

$$\text{exists a constant } \gamma > 0, \text{ such that } p_t^{\text{ItvPS}}(w_t, \mathcal{F}_t) \leq \gamma p_t(w_t, \mathcal{F}_t), \quad \forall w_t \in \{0, 1\}.$$

The common overlap assumption in causal inference literature requires that each time t has a positive probability of being treated or untreated. In contrast, a stochastic intervention framework may avoid the overlap assumption by not intervening at time points with zero probability of being either treated or untreated (Kennedy, 2019). Instead, the stochastic intervention framework only requires a weak overlap assumption to hold (Papadogeorgou *and others*, 2020). Specifically, the weak overlap assumption always holds under the proposed ItvPS intervention (a special type of stochastic intervention), since, according to Equation 2.1, $p_t^{\text{ItvPS}}(w_t, \mathcal{F}_t) \leq \max\{1, \delta_t\}p_t(w_t, \mathcal{F}_t)$, and $p_t^{\text{ItvPS}}(1, \mathcal{F}_t) \equiv 0$ when $p_t(1, \mathcal{F}_t) = 0$ and $p_t^{\text{ItvPS}}(0, \mathcal{F}_t) \equiv 0$ when $p_t(0, \mathcal{F}_t) = 0$ regardless of the value of δ_t (Naimi *and others*, 2021).

We now show that under the three assumptions defined above, our proposed causal estimand is identified.

At any time point $t \in \{1, \dots, T\}$,

$$\tau_t(\delta_{1:t}) = \sum_{w_{1:t} \in W_{1:t}} \int_{\partial \mathcal{R}_{1:t}} \mu(w_t, \mathcal{F}_t) \times \prod_{s=1}^t \underbrace{\left[\frac{w_s \delta_s p_s(1, \mathcal{F}_s) + (1 - w_s) \{1 - p_s(1, \mathcal{F}_s)\}}{\delta_s p_s(1, \mathcal{F}_s) + 1 - p_s(1, \mathcal{F}_s)} \right]}_{:= p_s^{\text{ItvPS}}(w_s, \mathcal{F}_s)} \times dPr(\partial r_s | W_{s-1} = w_{s-1}, \mathcal{F}_{s-1}),$$

where $\partial \mathcal{R}_{1:t} = \partial \mathcal{R}_1 \times \dots \times \partial \mathcal{R}_t$, $\partial \mathcal{R}_s = \mathcal{F}_s / \{\mathcal{F}_{s-1}, W_{s-1}\}$, $s = 1, \dots, t$, and $\mu(w_t, \mathcal{F}_t) = E(Y_t | W_t = w_t, \mathcal{F}_t)$.

However, although $\tau_t(\delta_{1:t})$ is causally identifiable, the corresponding quantity may not be stably estimated based on a single time series. We instead focus on the temporal average causal estimand

$$\bar{\tau}(\delta_{1:t,T}) = \frac{1}{T} \sum_{t=1}^T \tau_t(\delta_{1:t}),$$

which can also be causally identified given $\tau_t(\delta_{1:t})$ is identifiable $\forall t = 1, 2, \dots, T$. Likewise, the duration- t_0 causal estimand $\tau_t(\delta_{(t-t_0):t})$ and its temporal average counterpart $\bar{\tau}(\delta_{(t-t_0):t,T})$ can be identified under the same assumptions.

4. ESTIMATION AND INFERENCE

4.1 Weighted Estimation

We focus on the estimation and inference of duration- t_0 causal estimands $\tau_t(\delta_{(t-t_0):t})$ given the theoretical and practical conveniences discussed in Section 3.2. If the value of time-varying propensity score $p_s(1, \mathcal{F}_s)$ is known, as in Section 6 of Kim *and others* (2019), the unbiased estimator of $\tau_t(\delta_{(t-t_0):t})$ is defined as,

$$\hat{\tau}_t(\delta_{(t-t_0):t}) = \prod_{s=t-t_0}^t \left[\frac{\{W_s \delta_s + (1 - W_s)\}}{\underbrace{\delta_s p_s(1, \mathcal{F}_s) + 1 - p_s(1, \mathcal{F}_s)}_{:= p_s^{\text{ItvPS}}(W_s, \mathcal{F}_s) / p_s(W_s, \mathcal{F}_s)}} \right] Y_t.$$

When the time-varying propensity score $p_s(1, \mathcal{F}_s)$ is unknown, the estimation strategy requires two steps: 1) at each time s , we estimate the time-varying propensity score $\hat{p}_s(1, \mathcal{F}_s)$; 2) if the time-varying propensity scores can be modeled using correctly specified parametric models, we construct the following unbiased estimator for a duration- t_0 estimand on the observed treatment path,

$$\hat{\tau}_t(\delta_{(t-t_0):t}) = \prod_{s=t-t_0}^t \left[\frac{\{W_s \delta_s + (1 - W_s)\}}{\underbrace{\delta_s \hat{p}_s(1, \mathcal{F}_s) + 1 - \hat{p}_s(1, \mathcal{F}_s)}_{:= \hat{p}_s^{\text{I}t\text{vPS}}(w_s, \mathcal{F}_s) / \hat{p}_s(w_s, \mathcal{F}_s)}} \right] Y_t,$$

$$\hat{\hat{\tau}}_t(\delta_{(t-t_0):t,T}) = \frac{1}{T - t_0} \sum_{t=t_0+1}^T \hat{\tau}_t(\delta_{(t-t_0):t}) = \frac{1}{T - t_0} \sum_{t=t_0+1}^T \left(\prod_{s=t-t_0}^t \left[\frac{\{W_s \delta_s + (1 - W_s)\}}{\delta_s \hat{p}_s(1, \mathcal{F}_s) + 1 - \hat{p}_s(1, \mathcal{F}_s)} \right] Y_t \right).$$

The proposed estimator is defined as a weighted average of the observed outcomes Y_t weighted by time-varying weights, in which the weights correspond to the product of fractions where the numerators are $\hat{p}_s^{\text{I}t\text{vPS}}(w_s, \mathcal{F}_s)$ and denominators are $\hat{p}_s(w_s, \mathcal{F}_s)$. All estimators described above are generally referred to as “plug-in” estimators, since they take estimates for the time-varying propensity score $\hat{p}_s(1, \mathcal{F}_s)$, and plug it directly into the identifiable causal estimands.

4.2 Statistical Inference

We investigate the variance of the proposed “plug-in” estimators. For a fixed t , conditioning on \mathcal{F}_{t-t_0} , the variance of the estimator $\hat{\tau}_t(\delta_{(t-t_0):t})$ can be defined as

$$\text{Var}\{\hat{\tau}_t(\delta_{(t-t_0):t}) | \mathcal{F}_{t-t_0}\} = E \left(\underbrace{\prod_{s=t-t_0}^t \left[\frac{\{W_s \delta_s + (1 - W_s)\}}{\delta_s \hat{p}_s(1, \mathcal{F}_s) + 1 - \hat{p}_s(1, \mathcal{F}_s)} \right]^2 Y_t^2}_{\mathcal{V}_t} \middle| \mathcal{F}_{t-t_0} \right) - \left\{ E \left(\prod_{s=t-t_0}^t \left[\frac{\{W_s \delta_s + (1 - W_s)\}}{\delta_s \hat{p}_s(1, \mathcal{F}_s) + 1 - \hat{p}_s(1, \mathcal{F}_s)} \right] Y_t \middle| \mathcal{F}_{t-t_0} \right) \right\}^2,$$

where \mathcal{V}_t is defined as

$$\mathcal{V}_t = \sum_{w_{(t-t_0):t} \in W_{(t-t_0):t}} \int_{\partial \mathcal{R}_{(t-t_0):t}} E(Y_t^2 | W_{(t-t_0):t} = w_{(t-t_0):t}, \mathcal{F}_t) \times \prod_{s=t-t_0}^t \underbrace{\left[\frac{\{w_s \delta_s p_s(1, \mathcal{F}_s) + (1 - w_s) p_s(0, \mathcal{F}_s)\}}{\delta_s p_s(1, \mathcal{F}_s) + 1 - p_s(1, \mathcal{F}_s)} \right]^2}_{:= p_s^{\text{I}t\text{vPS}}(w_s, \mathcal{F}_s)^2} \times dPr(\partial r_s | W_{s-1} = w_{s-1}, \mathcal{F}_{s-1}).$$

The “plug-in” estimator of \mathcal{V}_t can be written as

$$\hat{\mathcal{V}}_t = \prod_{s=t-t_0}^t \left[\frac{\{W_s \delta_s^2 + (1 - W_s)\}}{[\delta_s \hat{p}_s(1, \mathcal{F}_s) + 1 - \hat{p}_s(1, \mathcal{F}_s)]^2} \right] Y_t^2. \quad (4.3)$$

A straightforward “plug-in” estimator of $Var\{\hat{\tau}_t(\delta_{(t-t_0):t})|\mathcal{F}_{t-t_0}\}$ can be written as

$$\widehat{Var}\{\hat{\tau}_t(\delta_{(t-t_0):t})|\mathcal{F}_{t-t_0}\} = \prod_{s=t-t_0}^t \left[\frac{\{W_s \delta_s^2 + (1 - W_s)\}}{[\delta_s \hat{p}_s(1, \mathcal{F}_s) + 1 - \hat{p}_s(1, \mathcal{F}_s)]^2} \right] Y_t^2 - \left(\prod_{s=t-t_0}^t \left[\frac{\{W_s \delta_s + (1 - W_s)\}}{[\delta_s \hat{p}_s(1, \mathcal{F}_s) + 1 - \hat{p}_s(1, \mathcal{F}_s)]} \right] Y_t \right)^2.$$

Note, this variance estimator on a single time series is always equal to 0, i.e.,

$$\begin{aligned} & \prod_{s=t-t_0}^t \left[\frac{\{W_s \delta_s^2 + (1 - W_s)\}}{[\delta_s \hat{p}_s(1, \mathcal{F}_s) + 1 - \hat{p}_s(1, \mathcal{F}_s)]^2} \right] Y_t^2 - \left(\prod_{s=t-t_0}^t \left[\frac{\{W_s \delta_s + (1 - W_s)\}}{[\delta_s \hat{p}_s(1, \mathcal{F}_s) + 1 - \hat{p}_s(1, \mathcal{F}_s)]} \right] Y_t \right)^2 \\ &= \left[\frac{\prod_{s=t-t_0}^t \delta_s^2}{\prod_{s=t-t_0}^t \{\delta_s \hat{p}_s(1, \mathcal{F}_s) + 1 - \hat{p}_s(1, \mathcal{F}_s)\}^2} \right] Y_t^2 - \left(\left[\frac{\prod_{s=t-t_0}^t \delta_s}{\prod_{s=t-t_0}^t \{\delta_s \hat{p}_s(1, \mathcal{F}_s) + 1 - \hat{p}_s(1, \mathcal{F}_s)\}} \right]^2 Y_t^2 \right) = 0. \end{aligned}$$

Therefore, instead, following the time series literature (Bojinov and Shephard, 2019; Papadogeorgou *and others*, 2020), we use \mathcal{V}_t as an upper bound of the conditional variance of $\hat{\tau}_t(\delta_{(t-t_0):t})$ conditioning on \mathcal{F}_{t-t_0} .

This is because we have

$$Var\{\hat{\tau}_t(\delta_{(t-t_0):t})|\mathcal{F}_{t-t_0}\} = \mathcal{V}_t - \left\{ E \left(\prod_{s=t-t_0}^t \left[\frac{\{W_s \delta_s + (1 - W_s)\}}{[\delta_s \hat{p}_s(1, \mathcal{F}_s) + 1 - \hat{p}_s(1, \mathcal{F}_s)]} \right] Y_t \middle| \mathcal{F}_{t-t_0} \right) \right\}^2 \leq \mathcal{V}_t,$$

and the “plug-in” estimator $\hat{\mathcal{V}}_t$ can be directly calculated using observed data as shown in Equation 4.3.

To calculate the variance of the temporal average estimator $\hat{\tau}(\delta_{(t-t_0):t,T}) = \frac{1}{T-t_0} \sum_{t=t_0+1}^T \hat{\tau}_t(\delta_{(t-t_0):t})$, we firstly define a sequence for the estimation error $u_{t,t_0} \equiv \hat{\tau}_t(\delta_{(t-t_0):t}) - \tau_t(\delta_{(t-t_0):t}), \forall t = 1, 2, \dots, T$ (t_0 is fixed). And then, we have $Var\{\hat{\tau}(\delta_{(t-t_0):t,T})\} = Var\{\frac{1}{T-t_0} \sum_{t=t_0+1}^T u_{t,t_0}\}$. Analogue to the proof of Theorem 1 in Bojinov and Shephard (2019) and Lemma 1 in Papadogeorgou *and others* (2020), u_{t,t_0} is a martingale difference sequence with respect to \mathcal{F}_{t-t_0} given u_{t,t_0} is bounded and $E(u_{t,t_0}|\mathcal{F}_{t-t_0}) = 0$. Consequently, the sequence u_{t,t_0} is uncorrelated through time t , and thus

$$\begin{aligned} Var\{\hat{\tau}(\delta_{(t-t_0):t,T})\} &= \frac{1}{(T-t_0)^2} \sum_{t=t_0+1}^T Var\{u_{t,t_0}\} = \frac{1}{(T-t_0)^2} \sum_{t=t_0+1}^T E[Var\{u_{t,t_0}|\mathcal{F}_{t-t_0}\}] \\ &= \frac{1}{(T-t_0)^2} \sum_{t=t_0+1}^T E[Var\{\hat{\tau}_t(\delta_{(t-t_0):t})|\mathcal{F}_{t-t_0}\}] \leq \frac{1}{(T-t_0)^2} \sum_{t=t_0+1}^T \mathcal{V}_t, \end{aligned}$$

and the “plug-in” estimator of an upper bound of $Var\{\hat{\tau}(\delta_{(t-t_0):t,T})\}$ can be expressed as $\frac{1}{(T-t_0)^2} \sum_{t=t_0+1}^T \hat{\mathcal{V}}_t$.

Using the martingale sequence property for the estimation error u_{t,t_0} , we can establish a central limit theorem (CLT) of the proposed estimators $\hat{\tau}(\delta_{(t-t_0):t,T})$ that allows us to build CIs.

Proposition 1 (Asymptotic Normality) Suppose that Assumptions 1–3 hold, if $\frac{1}{T-t_0} \sum_{t=t_0+1}^T E(u_{t,t_0}^2|\mathcal{F}_{t-t_0}) \xrightarrow{p} V^*$ for a positive constant V^* , then as $T \rightarrow \infty$, for a given t_0 we have,

$$\sqrt{T-t_0} \{ \hat{\tau}(\delta_{(t-t_0):t,T}) - \bar{\tau}(\delta_{(t-t_0):t,T}) \} = \sqrt{T-t_0} \left\{ \frac{1}{T-t_0} \sum_{t=t_0+1}^T u_{t,t_0} \right\} \xrightarrow{d} \mathcal{N}(0, V^*),$$

where $V^* = \lim_{T \rightarrow \infty} \frac{1}{(T-t_0)} \sum_{t=t_0+1}^T \text{Var}\{u_{t,t_0} | \mathcal{F}_{t-t_0}\}$.

The proof is provided in the Supplementary Materials Section S.1. Here, we note that an upper bound of V^* is $\lim_{T \rightarrow \infty} \frac{1}{(T-t_0)} \sum_{t=t_0+1}^T \mathcal{V}_t$. Then, we construct the confidence interval of $\hat{\tau}(\delta_{(t-t_0):t,T})$ as $\{\hat{\tau}(\delta_{(t-t_0):t,T}) - 1.96 \times \sqrt{\frac{1}{(T-t_0)^2} \sum_{t=t_0+1}^T \hat{\mathcal{V}}_t}, \hat{\tau}(\delta_{(t-t_0):t,T}) + 1.96 \times \sqrt{\frac{1}{(T-t_0)^2} \sum_{t=t_0+1}^T \hat{\mathcal{V}}_t}\}$.

5. META-ANALYSIS ON MULTI-SITE TIME SERIES

In many applications, time series data are available from multiple sites. In this section we generalize our ItvPS intervention framework to combine information from multi-site time series. To formalize the causal identification in the context of random-effects across multi-site time series, in Section 5.1 we introduce and discuss new assumptions of identification. In subsequent Section 5.2, we describe estimation and inference of the pooled estimator based on meta-analysis models.

5.1 Assumptions and Identification

There are at least two popular statistical models for meta-analysis, the fixed-effect model and the random-effects model (Borenstein *and others*, 2010). In general, we found the random-effects assumption is more plausible in many applications including our motivating example, allowing us to assume that the causal effects of heat alerts on health outcomes vary across counties. Therefore, we propose a meta-analysis method that relies on a random-effects model to obtain a pooled estimator to summarize the overall causal effect of time series data across multiple counties (DerSimonian and Laird, 2015).

Before introducing the new pooled estimator, we introduce additional assumptions to allow for causal inference that synthesizes evidence from multi-site time series. We use the index i to indicate the sites (i.e., counties in our motivating example), for $i \in \{1, 2, \dots, N\}$. We denote by $\mathcal{F}_t = \{\mathcal{F}_{1,t}, \dots, \mathcal{F}_{N,t}\}$ the filtration which captures the past information prior to time t in N sites.

Assumption 4 (Multi-site Time Series SUTVA) The multi-site outcome paths satisfy non-anticipating, non-interference, and consistency assumptions, that is, $Y_{i,t}^{\text{obs}} = Y_{i,t}(w_{1:N,1:T}^{\text{obs}}) = Y_{i,t}(w_{1:N,1:t}^{\text{obs}}) = Y_{i,t}(w_{i,1:t}^{\text{obs}}) \forall i = 1, \dots, N; t = 1, \dots, T$.

Assumption 4 generalizes Assumption 1 to the context of multi-sites. A notable constraint, beyond the non-anticipating and consistency in Assumption 1, is that the potential outcomes for one site are only affected by their own treatment path, and not by spillover effects across sites (non-interference).

Assumption 5 (Multi-site Time Series Unconfoundedness) The assignment mechanism is unconfounded if for all $W_{i,1:T} \in \mathcal{W} = \{0,1\}^T$, and $\mathcal{F}_t, W_{i,t} \perp Y_{i,s}(w_{i,1:s}) \mid \mathcal{F}_t \forall i = 1, \dots, N; t = 1, \dots, T$ and $t \leq s \leq T$.

Assumption 5 is similar to Assumption 2, which states the treatment path for each site depends on the past information only. This does not rule out the possibility that the probability of receiving the treatment on day t in one site could depend on covariates observed in another site prior to time t . There is no need to assume that the potential outcome in site i , $Y_{i,1:t}(w_{i,1:t})$, is independent from the potential outcome in a different site j , $Y_{j,1:t}(w_{j,1:t})$, for $i \neq j$.

Assumption 6 (Effect Independence across Multi-sites) Each site was given the same intervention path $\delta_{1:T}$, and the duration- t_0 causal estimands $\bar{\tau}_i(\delta_{(t-t_0):t})$ for site i are independent across $i = 1, \dots, N, \forall t = 1, \dots, T; t_0 = 1, \dots, t$.

Assumption 6 is a common assumption for meta-analysis (DerSimonian and Laird, 2015). This assumption consists of two components: first, we assume the causal estimands at each site are defined by the same ItvPS intervention $\delta_{1:T}$, and thus combining results in a meta-analysis is practically meaningful (e.g., one usually chooses to combine clinical studies of the same drug, rather than completely different drugs, in one meta-analysis); second, among the well-defined causal estimands $\bar{\tau}_i(\delta_{(t-t_0):t})$, we further assume effect independence across multi-sites. Such an effect independence assumption is commonly stated in random-effect meta-analysis models (DerSimonian and Laird, 2015), and was used in previous multi-site air pollution epidemiology studies (Bell *and others*, 2004).

We define a weighted average causal estimand across N sites, as the estimand of interest:

$$\bar{\tau}^N(\delta_{(t-t_0):t,T}) = \sum_{i=1}^N c_i \bar{\tau}_i(\delta_{(t-t_0):t,T}), \text{ where } \sum_{i=1}^N c_i = 1 \text{ and } \{c_i, i = 1, 2, \dots, N\} \text{ are fixed.}$$

Such a weighted causal estimand provides an overall summary of the causal effect drawn from a super-population, whereas the observations from each site are treated as a random sample from this super-population (DerSimonian and Laird, 2015). When Assumptions 4-6 hold, we show $\bar{\tau}^N(\delta_{(t-t_0):t,T})$ are causally

identified using a modified version of the identification equation from Section 3, that is, $\forall i \in \{1, 2, \dots, N\}$,

$$\begin{aligned} \tau_{i,t}(\delta_{1:t}) &= \sum_{w_{i,1:t} \in W_{i,1:t}} \int_{\partial \mathcal{R}_{1:t}} \mu(w_{i,t}, \mathcal{F}_t) \times \prod_{s=t-t_0}^t \underbrace{\frac{\{w_{i,s} \delta_s p_{i,s}(1, \mathcal{F}_{i,s}) + (1 - w_{i,s}) p_{i,s}(0, \mathcal{F}_s)\}}{\delta_s p_{i,s}(\mathcal{F}_s) + 1 - p_{i,s}(\mathcal{F}_s)}}_{:= p_{i,s}^{\text{tvPS}}(w_{i,s}, \mathcal{F}_s)} \\ &\quad \times dPr(\partial \mathbf{r}_s | W_{i,s-1} = w_{i,s-1}, \mathcal{F}_{s-1}), \\ \bar{\tau}_n(\delta_{(t-t_0):t,T}) &= \frac{1}{T-t_0} \sum_{t=t_0+1}^T \tau_{i,t}(\delta_{(t-t_0):t}), \quad \bar{\tau}^N(\delta_{(t-t_0):t,T}) = \sum_{i=1}^N c_i \bar{\tau}_i(\delta_{(t-t_0):t,T}). \end{aligned}$$

where $\partial \mathcal{R}_{1:t} = \partial \mathcal{R}_1 \times \dots \times \partial \mathcal{R}_t$, and $\partial \mathcal{R}_s = \mathcal{F}_s / \{\mathcal{F}_{s-1}, W_{i,s-1}\}$, $s = 1, \dots, t$, $\mu(w_{i,t}, \mathcal{F}_t) = E(Y_{i,t} | W_{i,t} = w_{i,t}, \mathcal{F}_t)$. $\{c_i, i = 1, 2, \dots, N\}$ are the fixed weights satisfying $\sum_{i=1}^N c_i = 1$. The remaining question is how to choose suitable weights c_i for each site i . To answer this question, we discuss a random-effects meta-analysis model in the following Section 5.2.

5.2 Estimation and Inference

The random-effects allow different sites to have heterogeneous causal effects that are sampled from a distribution characterizing the overall causal effect. The primary purpose is to make inferences about the pooled causal effect and provide a quantitative measure of how the causal effects differ across the sites. In the meta-analysis, to obtain a weighted average causal estimand that better characterizes the pooled causal effect synthesized from multiple sites, we assign more weight to sites that yield a more precise estimate of the overall causal effect. Random-effect models use an inverse variance scheme to assign weights to each site based on inverse proportions of the total variance from each site. Specifically, there are two sources of variance under a random-effects model (Borenstein *and others*, 2010). First, the observed causal effect $\hat{\tau}_i(\delta_{(t-t_0):t,T})$ for any time series in one site differs from that time series's true causal effect because of within-site variance, V_i . Second, the true causal effect for each time series differs from the overall causal effect because of between-site variance, τ^2 . Therefore, the weight assigned to each sites under the inverse variance scheme is

$$c_i = \frac{1}{V_i + \tau^2}, \quad i = 1, 2, \dots, N.$$

The within-site variance, V_i , is unique to each site, but the between-site variance τ^2 is a quantity that is common across sites.

6. SIMULATION STUDY

We study finite-sample properties of the proposed estimators via simulation studies on a single time series, in which we vary: a) the length of the time series T ; b) the duration of interventions t_0 ; and c) the assignment mechanisms of the treatment $p_t(W_t = 1 \mid \mathcal{F}_t)$. To reflect the nature of treatment assignment in our motivating example, we generate the treatment W_t under a nearly non-overlapping setting. In particular, we consider a time series with length T . For each $t = 1, \dots, T$,

$$\begin{aligned} \mathbf{C}_t &= (C_{1,t}, C_{2,t}, C_{3,t}, C_{4,t}, C_{5,t}) \sim N(\mathbf{0}, \mathbf{I}_5); \\ p_t(W_t = 1 \mid \mathcal{F}_t) &= \text{expit}\{10 \times (\sum_{j=1}^5 C_{j,t}/5 - W_{t-1} + 0.5)\}; \\ Y_t \mid W_t, W_{t-1}, \mathbf{C}_t &\sim N(3 \times W_t + W_{t-1} + \sum_{j=1}^5 C_{j,t}/5, 1). \end{aligned}$$

At time t , the random assignment mechanism of the treatment W_t depends on both \mathbf{C}_t , and the treatment at time $t - 1$, W_{t-1} . Also the outcome Y_t depends on the treatments both at time t and $t - 1$ (duration-1 effect). The data generating mechanism described above mimics a nearly non-overlap setting (see Figure S1 of the Supplementary Materials, showing the distributions of the time-varying propensity scores have little overlap across treated vs. untreated units). The main quantity of interest is the duration- t_0 causal estimand on the observed treatment path. We assess the performance of each estimator by calculating the integrated bias and root mean squared error (RMSE) defined as;

$$\begin{aligned} \widehat{\text{Integrated Bias}} &= \frac{1}{J} \sum_{j=1}^J \left| \frac{1}{K} \sum_{k=1}^K \{ \hat{\tau}^k(\delta_{t-t_0:t,T,j}) - \bar{\tau}^k(\delta_{t-t_0:t,T,j}) \} \right|, \\ \widehat{\text{RMSE}} &= \frac{\sqrt{N}}{J} \sum_{j=1}^J \left[\frac{1}{K} \sum_{k=1}^K \{ \hat{\tau}^k(\delta_{t-t_0:t,T,j}) - \bar{\tau}^k(\delta_{t-t_0:t,T,j}) \}^2 \right]^{1/2}, \end{aligned}$$

where $\bar{\tau}^k(\delta_{t-t_0:t,T,j}) := \frac{1}{T-t_0} \sum_{t=t_0+1}^T \bar{\tau}^k(\delta_{t-t_0:t,j})$ is the true temporal average causal quantity, and $\hat{\tau}^k(\delta_j)$ is its estimator based on the estimated time-varying propensity score, in which the superscript k indicates the simulation replicate. We assess the estimation performances at $J = 50$ values of δ_j equally spaced between 0.1 to 10 evaluated on $K = 500$ simulation replicates. We also assess the average coverage of our proposed 95% CIs.

We vary the following combinations of (T, t_0) , $T = (200, 1000, 5000)$, and $t_0 = (1, 4, 9)$. We apply both parametric and nonparametric models to estimate the time-varying propensity scores, following the recommendation by Bonvini *and others* (2021), 1) logistic regression; 2) Super Learner (Van der Laan *and others*,

2007), which combines generalized additive models, multivariate adaptive regression splines, support vector machines, and random forests, along with parametric generalized linear models (with and without interactions, and with terms selected stepwise via AIC), consistent with Kennedy (2019) (implemented by the **SuperLearner** R package). We assume that the form of the time-varying propensity score model is correctly specified as $W_t \mid \mathbf{C}_t, W_{t-1}$ with a **logit** link. We conduct additional simulations in the Supplementary Materials to show the results when the form of the time-varying propensity score model is misspecified.

Table 2 shows the proposed estimator performs well in various settings. Under the same duration t_0 , we observed that the integrated bias and RMSE of the estimator decreases when the length of the time series, T , increases, regardless of how the time-varying propensity score is estimated, either by logistic regression or Super Learner. We also observed a decreased performance of the estimator as the duration, t_0 , increases. This finding is not surprising given that the estimated weights in the proposed weighting estimator depend on the product of $t_0 + 1$ terms of estimated ItvPS. We expect that the proposed estimator will likely be unstable and thus the absolute bias and RMSE will be larger when t_0 increases. In practice the exact duration t_0 is unknown and researchers need to specify t_0 based on their prior domain knowledge. The simulation results suggest that the choice of t_0 should be parsimonious, that is, one should choose a duration t_0 that can capture the data complexity yet is as small as possible. We also found that using the Super Learner model to estimate the time-varying propensity score leads to improved performances compared to the logistic regression model even if the propensity score model is correctly specified with a **logit** link. This finding suggests that the Super Learner, as an ensemble of flexible parametric/nonparametric models, is competent in various settings. Additional simulations in the Supplementary Materials indicate promising performances of the Super Learner when the underlying data generating mechanism is unknown and potentially complex.

We also found that the average coverage was near or above the nominal level (95%) when T is relatively large, as shown in Table 2. The conservative performance is likely due to the fact that we used an upper bound for the variance estimates when constructing the CIs. The coverage decreases when t_0 increases, which is consistent with the coverage results shown in Papadogeorgou *and others* (2020). Figure 2 further shows the curve of duration-1 causal effects when the probability of the treatment assignment are multiplied by odds ratios $\delta_t \in [0.1, 10]$. The red solid line represents the estimated causal effects along with point-wise 95% point-wise confidence bands (red dashed line). We found that the bias between the estimated curve and

the true curve reduces when T increases. The point-wise 95% confidence bands capture the true curve in all three scenarios; $T = 200, 1000, 5000$.

We design our simulation studies to reflect a nearly non-overlap scenario, reflecting the nearly non-overlap between treated and untreated units observed in our data application. Our simulation results show that the proposed estimators perform well in terms of bias and root mean squared error even when the overlap assumption is nearly violated.

7. APPLICATION

We analyze the multi-site time series data described in Section 2.2. First, we apply the proposed methods to estimate the causal estimands $\bar{\tau}_i(\delta_{(t-t_0):t,T})$. We assume δ_t is the same for every day t during the warm months (April-October) of 2006-2016.

In the time-varying propensity score model, we included the following observed covariates: daily maximum heat index, lag-1 daily maximum heat index, lag-2 daily maximum heat index, moving average heat index during the current warm season, lag-1 day heat alert, lag-2 day heat alert, the running total number (the summation of the sequence of numbers updated daily) of heat alerts that have been issued during the current warm season, the moving average number of deaths/hospitalizations during the current warm season, day of the week, and federal holidays. Note, as described in Section 2.2, the inclusion of past treatments (lagged heat alerts) and past outcomes (historical deaths/hospitalizations) is allowed in the time-varying propensity score model. The time-varying propensity score was estimated a Super Learner using the same combination of algorithms described in Section 6.

For each county i , we estimate the daily numbers of all-cause deaths and cause-specific hospitalizations for five heat-related diseases (heat stroke, urinary tract infections, septicemia, renal failure, fluid and electrolyte disorders) under several ItvPS intervention scenarios ranging from $\delta_t = 0.1$ to $\delta_t = 10$. We consider the causal estimands with duration $t_0 = 2$, consistent with Weinberger *and others* (2018). We define the county-specific causal effect curve for county i as $\bar{\tau}_i(\delta_{(t-2):t,T}) - \bar{\tau}_i(1, 1, 1)$, where $\bar{\tau}_i(\delta_{(t-2):t,T})$ denotes the estimated daily average number of deaths or hospitalizations under various ItvPS interventions ($\delta_t \in [0.1, 10]$) and $\bar{\tau}_i(1, 1, 1)$ denotes the quantity corresponding to the daily average number of deaths or hospitalizations observed *factually* (as if there was no change in the treatment assignments). After obtaining all $N = 2, 837$ county-specific causal effect curves, we utilize the meta-analysis approach proposed in Section 5 to pool

the estimated county-specific causal effect curves across multiple counties, and obtain the estimated pooled causal effect curve, $\sum_{i=1}^N c_i [\bar{\tau}_i(\delta_{(t-2):t,T}) - \bar{\tau}_i(1, 1, 1)]$, where the weights $c_i, i = 1, 2, \dots, N$ are obtained by the random-effects meta-analysis model.

Figure 3 shows the estimated pooled causal effects for the daily average number of all-cause deaths and cause-specific hospitalizations for five heat-related diseases per county among 2,837 counties across the warm months of 2006-2016. The curves represent the differences in daily average numbers of deaths and hospitalizations averaged across 2,837 counties comparing the counterfactual scenarios where the probability of issuing heat alerts were multiplied by an odds ratio $\delta_t \in [0.1, 10]$ to the factual scenario, where the probability of issuing heat alerts remains unchanged ($\delta_t = 1$). The dotted lines present the corresponding point-wise 95% confidence bands of the differences. The black vertical lines represent the average number of deaths and hospitalizations that could be avoided per day per county and their corresponding CIs if we had increased the probability of issuing heat alerts by the maximum odds considered, $\delta_t = 10$. We find, in general, consistent downward patterns among the pooled causal effect curves for each health outcome as the $\log(\delta_t)$ increases above 0, indicating slight reductions of average all-cause deaths and cause-specific hospitalizations for five heat-related diseases among Medicare enrollees as $\log(\delta_t)$ increases. The curves are relatively flat, especially when $\log(\delta_t) < 0$, and also the CIs contain 0 throughout the range of $\delta_t \in [0.1, 10]$.

Quantitatively, we found that if we had increased the probability of issuing heat alerts by an odds ratio $\delta_t = 10$, on average 0.08 (95% CI: -0.02 to 0.17) deaths could be averted per day per county (see vertical black line in Figure 3a). Based on these estimates, solely among extremely hot days (i.e., the top 5% hottest days when the heat alerts are more likely to be issued), we estimated 2,329 avoidable deaths (95% CI: -510 to $5,168$) across all 2,837 counties in one warm season. Similarly, if we increase the probability of issuing heat alerts by an odds ratio $\delta_t = 10$ the number of hospitalizations avoided are 207 (95% CI: -122 to 536) for heat stroke; 2,508 (95% CI: $-2,110$ to $7,126$) for urinary tract infections; 4,674 (95% CI: $-4,229$ to $13,576$) for septicemia; 2,164 (95% CI: $-1,642$ to $5,969$) for renal failure; 1,733 (95% CI: $-1,235$ to $4,702$) for fluid and electrolyte disorders among extremely hot days in one warm season. However, given the wide confidence bands for the results of all outcomes, we do not find any statistically significant results of the causal effects of multiplying the probability of issuing heat alerts on health outcomes comparing $\delta_t = 10$ (increased odds) vs. $\delta_t = 1$ (unchanged). We also find there is large

between-county heterogeneity in the random-effects meta-analysis model, (P-value of heterogeneity test < 0.001), for all outcomes. Overall, our findings suggest weak evidence that increasing the probability of issuing heat alerts may bring health benefits to the U.S. Medicare population.

As a sensitivity analysis in the Supplementary Materials, we analyzed a subset of 550 counties with population sizes $> 100,000$ (“populous counties”). These counties included more than 70% of all-cause deaths and cause-specific hospitalizations observed among the 2,837 counties. The motivation for this additional sensitivity analysis was the concern that combining counties with varying population sizes introduces too much heterogeneity in the pooled causal estimates. As shown in Section S.3, the shapes of the causal effect curves based on the subset of 550 populous counties are very similar to the estimated curves based on data from all 2,837 counties. We found non-significant results for all outcomes. However, the width of confidence bands is generally narrower than those based on all 2,837 counties, which indicates reduced heterogeneity. Yet the random-effects meta-analysis model still indicates considerable between-county heterogeneity (P-value of heterogeneity test < 0.001) for all outcomes.

Additional analysis was conducted in which the duration of interventions was varied. We estimated pooled causal effect curves of duration-0 and duration-5 estimands. As shown in Supplementary Materials Section S.3, the causal effect of increasing the frequency of issuing heat alerts may have more pronounced effects on health outcomes when considering longer duration of interventions. Importantly, we observed statistically significant results of the causal effects of multiplying the probability of issuing heat alerts on health outcomes comparing $\delta_t = 10$ (increased odds) vs. $\delta_t = 1$ (unchanged) when considering cumulative effects up to duration $t_0 = 5$, i.e., on average 0.15 (95% CI: 0.06 to 0.24) avoidable deaths per day per county. We also found the widths of CIs for the causal effect curves of duration-0, duration-2 and duration-5 estimands did not change notably as t_0 varies.

8. DISCUSSION

We have developed a novel causal inference framework for multi-site time series data that relies on stochastic interventions. Under this framework, we introduced a class of causal estimands and their unbiased estimators with theoretical justification. In the context of multi-site time series data, we link our ItvPS intervention framework to the random-effects meta-analysis framework. The ultimate goal in this setting is to obtain a

pooled causal estimator that summarizes the potentially heterogeneous causal effects obtained from multi-site time series studies.

Our approach was motivated by our data application, where the goal was to assess whether or not increasing the probability of issuing heat alerts reduces morbidity and mortality. More specifically, we estimated the causal effects of increasing the probability of issuing heat alerts on all-cause deaths and cause-specific hospitalizations for five heat-related diseases. We found some evidence of reductions in morbidity and mortality with large statistical uncertainty. Importantly, the random-effects meta-analysis model indicated large heterogeneity of the causal effects across different counties.

One key distinction of our approach compared to more traditional statistical methods in environmental epidemiology, is that most time series studies in this context use matched case-crossover or difference-in-difference designs, where the focus is often the (average) causal contrast between treated days (i.e., days with heat alerts) vs. untreated days (i.e., days without heat alerts), and the number of heat alert days is then fixed for a given study period in one chosen site by the study design (Chau *and others*, 2009; Weinberger *and others*, 2018, 2021). In contrast, our analysis focuses on the causal effect of a stochastic intervention, estimating the causal effect as the probability of issuing heat alerts changes, and as such, the counterfactual heat alert days are not fixed. Therefore our results are not directly comparable to previously published studies (Weinberger *and others*, 2021).

While our proposed novel causal inference approach provides a new powerful tool in policy evaluations, some methodology considerations are needed when applying this approach to future studies. First, we expect causal effects defined by stochastic interventions to answer a different policy question than that of a deterministic intervention (Kennedy, 2019). The proposed causal estimand is an intuitive quantity answering the following causal question “how many adverse health outcomes could have been averted if we change the frequency of heat alerts?” which was the focus of our work. However, other practitioners’ interests may be more aligned with estimating causal effects of deterministic interventions, for instance, “how many adverse health outcomes could have been avoided if the temperature was, on average, one degree lower during extremely hot days (Weinberger *and others*, 2020)?” In that case, causal inference methods based on deterministic interventions (Bojinov and Shephard, 2019; Bojinov *and others*, 2020; Rambachan and Shephard, 2021) may be used. Second, the ItvPS intervention framework is flexible on the magnitude of intervention δ_t and the way

the intervention being executed. In particular, practitioners can incorporate data-dependent time-varying δ_t rather than a fixed δ_t throughout time (Bonvini *and others*, 2021), or execute more complex intervention strategies, such as an intervention strategy that optimizes the overall health benefit under pre-determined constraints on the number of heat alerts. The ItvPS intervention considered should be closely related to policy questions and goals. Third, the random-effects meta-analysis creates a weighted average causal estimand and its corresponding pooled estimator, in which the weights are calculated by combining between-site and within-site variance. For this reason, the weighted average causal quantity is defined on a hypothetical weighted population. Dahabreh *and others* (2020) have criticized that standard meta-analyses may produce results that do not belong to a clear target population when each site represents a different population and the treatment effect varies across these populations. As part of future work, we plan to develop approaches that allow inferences to be transported from multi-site time series to a clearly specified target population (Li and Song, 2020; Dahabreh *and others*, 2020). Fourth, the non-interference assumption may not hold in many climate and health studies, such as this one, which rely on spatial-temporal data. For instance, the NWS-issued heat alerts in one county may impact people in adjacent counties. As part of future work, we hope to extend the time series intervention path to a multivariate intervention path defined by random matrices (Papadogeorgou *and others*, 2020), to potentially overcome the violation of non-interference assumption, and identify direct and spillover effects under this stochastic intervention framework. Fifth, the stable estimation of time-varying propensity score based on time series observational data is challenging since the time-varying confounder sets are potentially high-dimensional. While in our data application we used the state-of-art Super Learner (an ensemble of flexible parametric/nonparametric models) to estimate time-varying propensity scores, we had to limit the size of confounder sets to avoid unstable estimates due to curse of dimensionality. Also, the proposed weighting estimator relying on products of the estimated ItvPS may be unstable when accounting for the longer duration of interventions. We plan to generalize covariate balance methods to improve high-dimensional propensity score estimation and stability of the weighting estimators in time series observational studies (Imai and Ratkovic, 2014; Athey *and others*, 2018).

The stochastic intervention framework for time series data introduced in this paper is the first approach that allows the identification and estimation of causal quantities defined by stochastic interventions on multi-site time series. We believe this framework addresses one of the emerging methodological needs in climate and

health research, where researchers often collect time series data from multiple geographic locations seeking causal evidence among diverse populations (Liu *and others*, 2019; Lee *and others*, 2020). Furthermore, we expect the proposed framework can be applied to science and policy-relevant research in political science, economics, and law, where a considerable amount of spatial-temporal data are generated and collected.

ACKNOWLEDGEMENT

The authors are grateful to Jose R. Zubizarreta, Ambarish Chattopadhyay, Eli Ben-Michael, Kosuke Imai, and Guanbo Wang for helpful discussions. Funding was provided by the National Institute of Health (NIH) grants R01 ES029950, R01 AG066793-01R01, R01 ES030616, R01 AG060232-01A1, R01 ES028033, R01 MD012769, R01 ES026217, F32-ES027742; USEPA grants 83587201-0; grant 216033-Z-19-Z from the Wellcome Trust, and Harvard University Climate Change Solutions Fund. The funders had no role in considering the study design or in the collection, analysis, interpretation of data, writing of the report, or decision to submit the article for publication. Dr. Wellenius and Dr. Dominici have received consulting income from the Health Effects Institute (Boston, MA). Dr. Wellenius recently served as a visiting scientist at Google, LLC (Mountain View, CA). The authors report that they have no conflicts of interest relevant to this work.

REFERENCES

- ATHEY, SUSAN, IMBENS, GUIDO W AND WAGER, STEFAN. (2018). Approximate residual balancing: debiased inference of average treatment effects in high dimensions. *Journal of the Royal Statistical Society: Series B (Statistical Methodology)* **80**(4), 597–623.
- BELL, MICHELLE L, SAMET, JONATHAN M AND DOMINICI, FRANCESCA. (2004). Time-series studies of particulate matter. *Annu. Rev. Public Health* **25**, 247–280.
- BHASKARAN, KRISHNAN, GASPARRINI, ANTONIO, HAJAT, SHAKOOR, SMEETH, LIAM AND ARMSTRONG, BEN. (2013). Time series regression studies in environmental epidemiology. *International journal of epidemiology* **42**(4), 1187–1195.
- BOBB, JENNIFER F, OBERMEYER, ZIAD, WANG, YUN AND DOMINICI, FRANCESCA. (2014). Cause-specific risk of hospital admission related to extreme heat in older adults. *Jama* **312**(24), 2659–2667.

- BOJINOV, IAVOR, RAMBACHAN, ASHESH AND SHEPHARD, NEIL. (2020). Panel experiments and dynamic causal effects: A finite population perspective. *arXiv preprint arXiv:2003.09915*.
- BOJINOV, IAVOR AND SHEPHARD, NEIL. (2019). Time series experiments and causal estimands: exact randomization tests and trading. *Journal of the American Statistical Association*, 1–36.
- BONVINI, MATTEO, MCCLEAN, ALEC, BRANSON, ZACH AND KENNEDY, EDWARD H. (2021). Incremental causal effects: an introduction and review. *arXiv preprint arXiv:2110.10532*.
- BORENSTEIN, MICHAEL, HEDGES, LARRY V, HIGGINS, JULIAN PT AND ROTHSTEIN, HANNAH R. (2010). A basic introduction to fixed-effect and random-effects models for meta-analysis. *Research synthesis methods* **1**(2), 97–111.
- CHAU, PH, CHAN, KC AND WOO, JEAN. (2009). Hot weather warning might help to reduce elderly mortality in hong kong. *International journal of biometeorology* **53**(5), 461–468.
- DAHABREH, ISSA J, PETITO, LUCIA C, ROBERTSON, SARAH E, HERNÁN, MIGUEL A AND STEINGRIMSSON, JON A. (2020). Toward causally interpretable meta-analysis: Transporting inferences from multiple randomized trials to a new target population. *Epidemiology* **31**(3), 334–344.
- DERSIMONIAN, REBECCA AND LAIRD, NAN. (2015). Meta-analysis in clinical trials revisited. *Contemporary clinical trials* **45**, 139–145.
- GRANGER, CLIVE WJ. (1980). Testing for causality: a personal viewpoint. *Journal of Economic Dynamics and control* **2**, 329–352.
- HANEUSE, SEBASTIAN AND ROTNITZKY, ANDREA. (2013). Estimation of the effect of interventions that modify the received treatment. *Statistics in medicine* **32**(30), 5260–5277.
- HAWKINS, MICHELLE D, BROWN, VANKITA AND FERRELL, JANNIE. (2017). Assessment of noaa national weather service methods to warn for extreme heat events. *Weather, climate, and society* **9**(1), 5–13.
- IMAI, KOSUKE AND JIANG, ZHICHAO. (2019). Comment: The challenges of multiple causes. *Journal of the American Statistical Association* **114**(528), 1605–1610.

- IMAI, KOSUKE AND RATKOVIC, MARC. (2014). Covariate balancing propensity score. *Journal of the Royal Statistical Society: Series B (Statistical Methodology)* **76**(1), 243–263.
- IMBENS, GUIDO W AND RUBIN, DONALD B. (2015). *Causal inference in statistics, social, and biomedical sciences*. Cambridge University Press.
- KANG, JOSEPH DY, SCHAFER, JOSEPH L *and others*. (2007). Demystifying double robustness: A comparison of alternative strategies for estimating a population mean from incomplete data. *Statistical science* **22**(4), 523–539.
- KENNEDY, EDWARD H. (2019). Nonparametric causal effects based on incremental propensity score interventions. *Journal of the American Statistical Association* **114**(526), 645–656.
- KIM, KWANGHO, KENNEDY, EDWARD H AND NAIMI, ASHLEY I. (2019). Incremental intervention effects in studies with many timepoints, repeated outcomes, and dropout. *arXiv preprint arXiv:1907.04004*.
- LEE, WHANHEE, KIM, YOONHEE, SERA, FRANCESCO, GASPARRINI, ANTONIO, PARK, ROKJIN, CHOI, HAYON MICHELLE, PRIFTI, KRISTI, BELL, MICHELLE L, ABRUTZKY, ROSANA, GUO, YUMING *and others*. (2020). Projections of excess mortality related to diurnal temperature range under climate change scenarios: a multi-country modelling study. *The Lancet Planetary Health* **4**(11), e512–e521.
- LI, XIHAO AND SONG, YANG. (2020). Target population statistical inference with data integration across multiple sources—an approach to mitigate information shortage in rare disease clinical trials. *Statistics in Biopharmaceutical Research* **12**(3), 322–333.
- LIU, CONG, CHEN, RENJIE, SERA, FRANCESCO, VICEDO-CABRERA, ANA M, GUO, YUMING, TONG, SHILU, COELHO, MICHELINE SZS, SALDIVA, PAULO HN, LAVIGNE, ERIC, MATUS, PATRICIA *and others*. (2019). Ambient particulate air pollution and daily mortality in 652 cities. *New England Journal of Medicine* **381**(8), 705–715.
- NAIMI, ASHLEY I, RUDOLPH, JACQUELINE E, KENNEDY, EDWARD H, CARTUS, ABIGAIL, KIRKPATRICK, SHARON I, HAAS, DAVID M, SIMHAN, HYAGRIV AND BODNAR, LISA M. (2021). Incremental propensity score effects for time-fixed exposures. *Epidemiology* **32**(2), 202–208.

- PAPADOGEORGOU, GEORGIA, IMAI, KOSUKE, LYALL, JASON AND LI, FAN. (2020). Causal inference with spatio-temporal data: Estimating the effects of airstrikes on insurgent violence in iraq. *arXiv preprint arXiv:2003.13555*.
- RAMBACHAN, ASHESH AND SHEPHARD, NEIL. (2021). When do common time series estimands have non-parametric causal meaning?
- ROBINS, JAMES M, ROTNITZKY, ANDREA AND ZHAO, LUE PING. (1994). Estimation of regression coefficients when some regressors are not always observed. *Journal of the American statistical Association* **89**(427), 846–866.
- ROSENBAUM, PAUL R AND RUBIN, DONALD B. (1983). The central role of the propensity score in observational studies for causal effects. *Biometrika* **70**(1), 41–55.
- US EPA, ENVIRONMENTAL PROTECTION AGENCY. (2006). Excessive heat events guidebook.
- VAN DER LAAN, MARK J, POLLEY, ERIC C AND HUBBARD, ALAN E. (2007). Super learner. *Statistical applications in genetics and molecular biology* **6**(1).
- WEINBERGER, KATE R, HARRIS, DANIEL, SPANGLER, KEITH R, ZANOBETTI, ANTONELLA AND WELLENIUS, GREGORY A. (2020). Estimating the number of excess deaths attributable to heat in 297 united states counties. *Environmental Epidemiology* **4**(3), e096.
- WEINBERGER, KATE R, WU, XIAO, SUN, SHENGZHI, SPANGLER, KEITH R, NORI-SARMA, AMRUTA, SCHWARTZ, JOEL, REQUIA, WEEBERB, SABATH, BENJAMIN M, BRAUN, DANIELLE, ZANOBETTI, ANTONELLA *and others*. (2021). Heat warnings, mortality, and hospital admissions among older adults in the united states. *Environment International* **157**, 106834.
- WEINBERGER, KATE R, ZANOBETTI, ANTONELLA, SCHWARTZ, JOEL AND WELLENIUS, GREGORY A. (2018). Effectiveness of national weather service heat alerts in preventing mortality in 20 us cities. *Environment international* **116**, 30–38.

Table 1: Characteristics for NWS-issued heat alerts, all-cause deaths among Medicare enrollees, and cause-specific hospitalizations for five heat-related diseases among Medicare FFS enrollees across April-October of 2006-2016.

Variables	2, 837 Counties	550 Populous Counties ¹
% Days with Heat Alerts	2.52 %	2.22 %
# of Deaths	10,467,201	7,653,987
# of Heat stroke	97,399	72,649
# of Urinary tract infections	1,424,046	1,061,060
# of Septicemia	2,614,871	1,954,011
# of Renal failure	1,207,903	894,164
# of Fluid and electrolyte disorders	928,270	673,007

1. Counties with population > 100,000.

Table 2: Simulation results for the scenario assuming the treatment assignment mechanism is specified with a **logit** link. The integrated bias and root mean squared error (RMSE) (multiplied by 10 for easier interpretation) of proposed estimators, and the average coverage of proposed confidence intervals (CIs).

Propensity Score Model	T	t_0	Integrated Bias	RMSE	Average Coverage (%)	
Logistic Regression	200	1	1.34	1.57	99.97	
		4	2.95	3.15	97.80	
		9	5.57	5.73	89.58	
	1000	1	0.25	0.45	100.00	
		4	0.59	0.74	99.98	
		9	1.06	1.18	96.45	
	5000	1	0.12	0.20	100.00	
		4	0.30	0.35	100.00	
		9	0.60	0.64	97.68	
	Super Learner	200	1	1.08	1.33	99.64
			4	2.24	2.46	95.49
			9	4.11	4.30	90.89
1000		1	0.04	0.34	100.00	
		4	0.08	0.38	99.99	
		9	0.21	0.49	99.41	
5000		1	0.04	0.16	100.00	
		4	0.14	0.24	99.97	
		9	0.33	0.42	99.19	

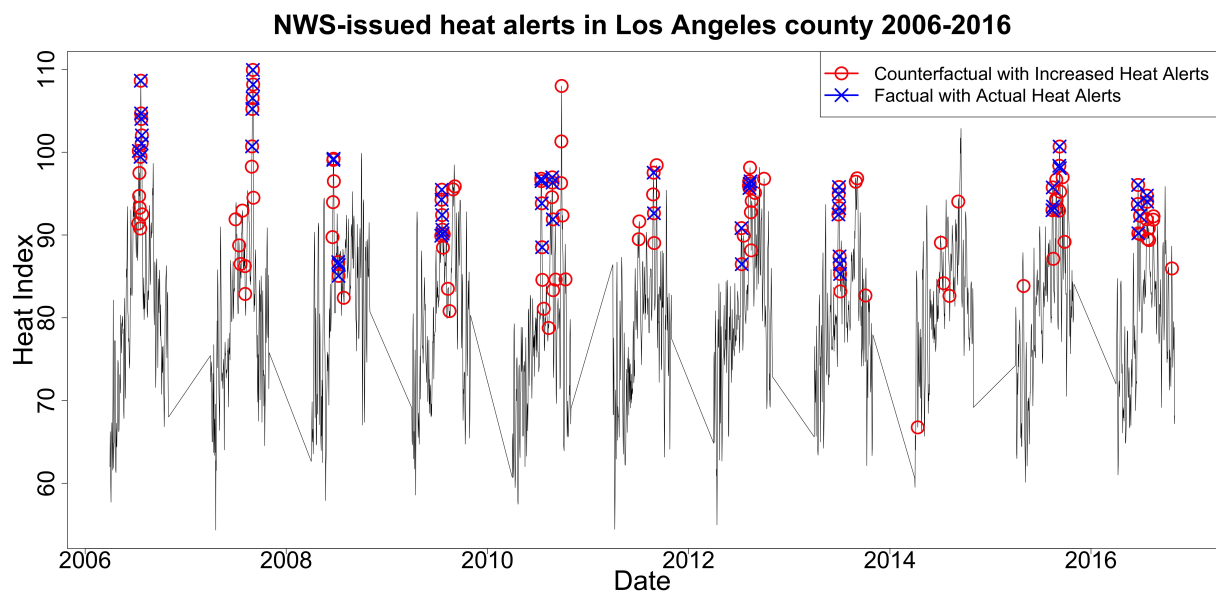


Fig. 1: NWS-issued heat alerts for Los Angeles County during the warm months (April-October) of 2006-2016. The blue x's represent the heat alerts that were issued *factually*, and the red circles represent the anticipated heat alerts under a counterfactual scenario where the probability of issuing heat alerts were increased for every warm-season day by an odds ratio 10. Therefore, we find under this counterfactual scenario, Los Angeles County would have issued 128 heat alerts from 2006-2016, compared to 56 heat alerts that were actually issued.

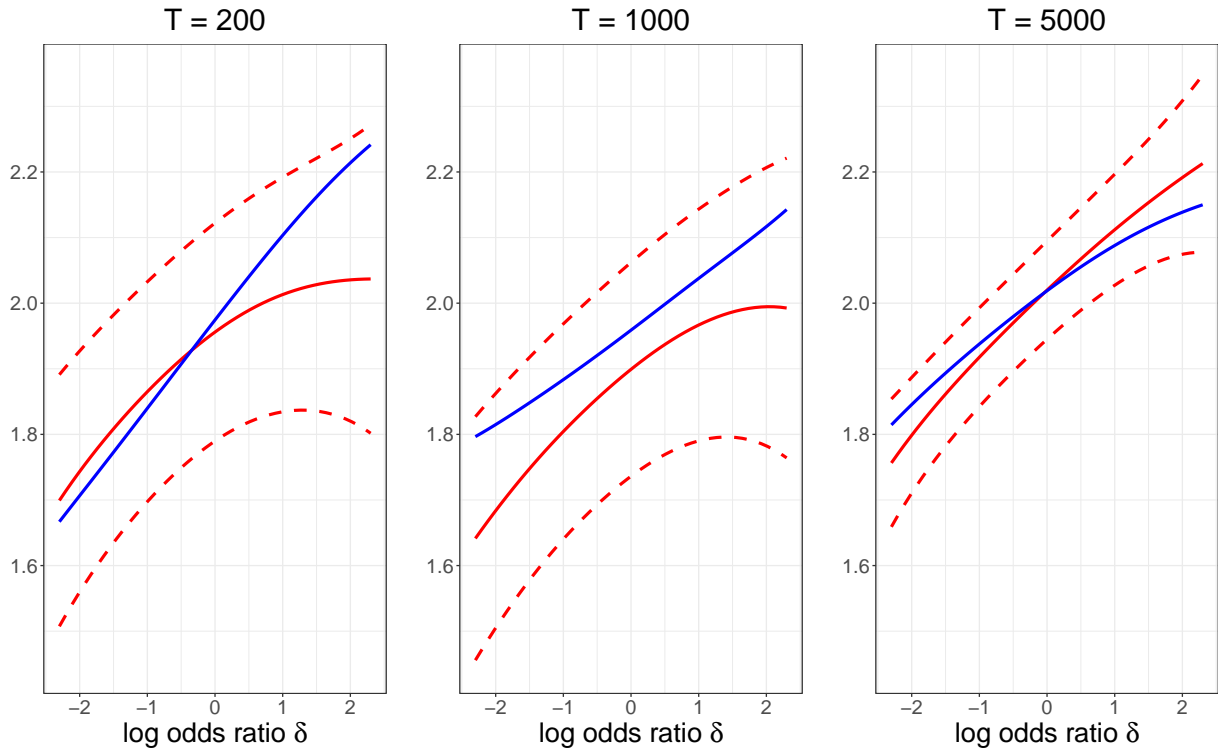


Fig. 2: The duration-1 causal effect curves when the probability of treatment assignments were multiplied by an odds ratio $\delta_t \in [0.1, 10]$. The red solid line represents the estimated causal effect curve along with the point-wise 95% Wald confidence band (red dashed line). The blue solid line represents the true causal effect curve. The left, middle and right panels reflect the simulation scenarios with $T = 200, 1000, 5000$. The propensity scores were estimated by a Super Learner algorithm including generalized additive models, multivariate adaptive regression splines, support vector machines, and random forests, along with parametric generalized linear models (with and without interactions, and with terms selected stepwise via AIC), consistent with Kennedy (2019).

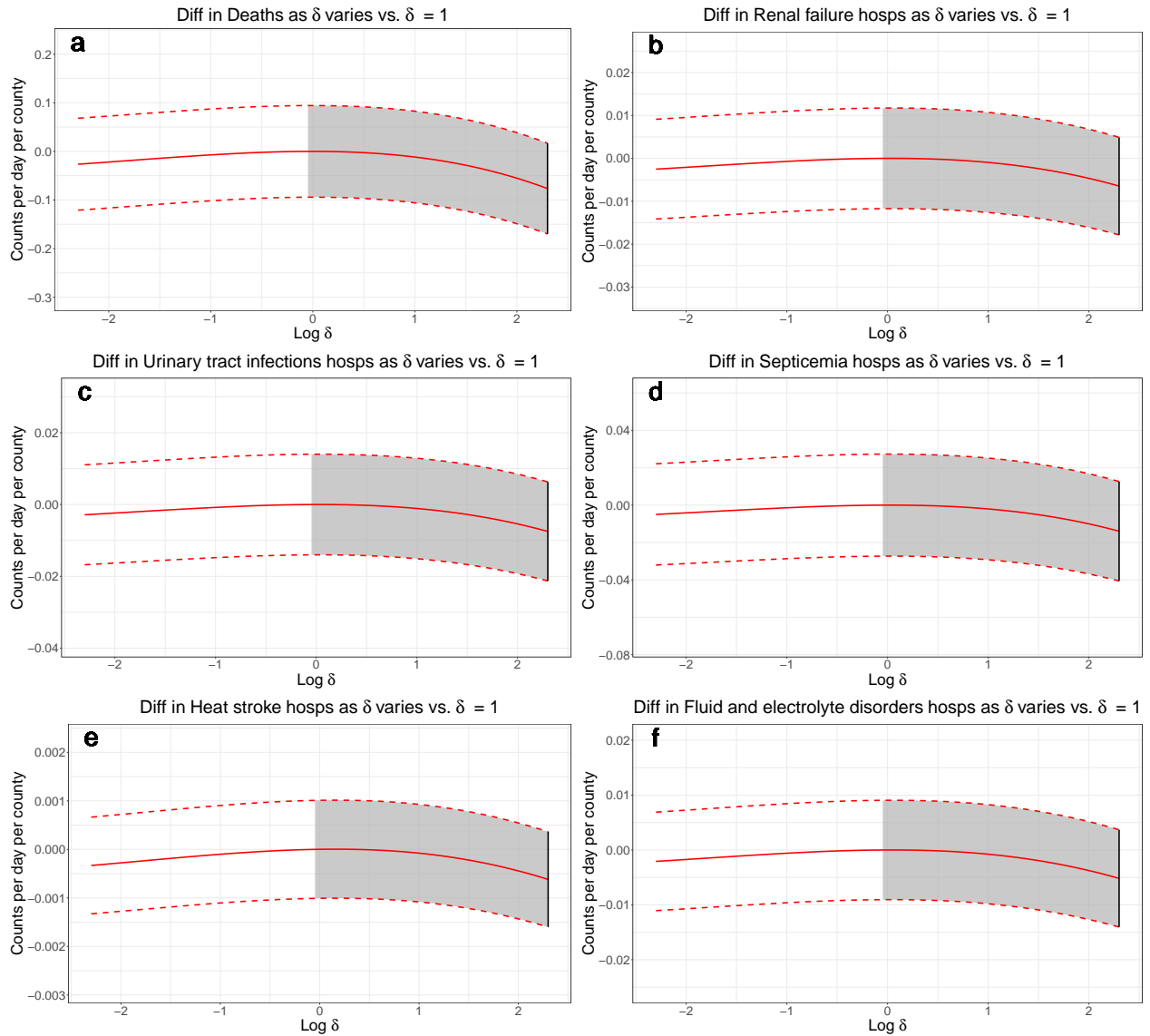


Fig. 3: The estimated pooled duration-2 causal effect curves of average all-cause deaths and cause-specific hospitalizations for five heat-related diseases per day per county among 2,837 counties. The curves represent the differences in deaths and hospitalizations comparing the counterfactual situations where the probability of issuing heat alerts were multiplied by an odds ratio $\delta_t \in [0.1, 10]$ to the factual situations where the probability of issuing heat alerts remains unchanged ($\delta_t = 1$). The dotted lines present the corresponding point-wise 95% confidence bands of the differences. The black vertical lines represent the daily average number of deaths and hospitalizations that could be avoided for a county and their corresponding confidence intervals (CIs) if we had increased the probability of issuing heat alerts by an odds ratio $\delta_t = 10$.